Preparation and Characterization of Cross-Linked Polymeric Nanoparticles for Enhanced Oil Recovery Applications

Nodar Al-Manasir, Anna-Lena Kjøniksen, Bo Nyström

Department of Chemistry, University of Oslo, Blindern, Oslo N-0315, Norway

Received 11 December 2008; accepted 30 January 2009
DOI 10.1002/app.30176
Published online 17 April 2009 in Wiley InterScience (www.interscience.wiley.com).

ABSTRACT: Chemically cross-linked nanoparticles from dilute aqueous alkali solutions of hydroxyethylcellulose (HEC) in the presence of a cross-linker agent (divinyl sulfone, DVS) were prepared from a reaction mixture, which was exposed to different stirring speeds during the cross-linking process. At various stages during the cross-linking procedure, the reaction was terminated and the species were characterized by means of turbidimetry, asymmetric flow field-flow fractionation (AFFFF), dynamic light scattering (DLS), and rheo-small-angle light scattering (rheo-SALS) methods. During the cross-linking of a dilute polymer solution, the competition between intrapolymer and interpolymer is a prominent feature. The DLS results show that at early times in the cross-linking process, intrachain cross-linking with contraction of the complexes is promoted by high stirring speeds; at later times the growth of aggregates is inhibited by high stirring speeds. The results from the rheo-SALS measurements disclosed that at early times during the cross-linker reaction, the complexes are fragile against shear forces if the reaction mixture had been subjected to low stirring speeds. At a later state of cross-linking, more cross-links lead to better stability of the species, even for solutions that have been exposed to low stirring speeds during the cross-linking process. This study shows that the sizes of the particles can be tuned by exposing the solutions to different stirring speeds during the cross-linker reaction and to terminate the reaction at desired reaction times. The strategy discussed in this work for the preparation of particles of various sizes is of special interest in connection with enhanced oil recovery applications. J Appl Polym Sci 113: 1916–1924, 2009

Key words: cross-linking; biopolymers; dynamic light scattering; microgels; polysaccharides

INTRODUCTION

It has been known for some time that some polymers provide good handling characteristics and solubility to enhance injection properties through reservoir permeability. Polymers are frequently used in enhanced oil recovery (EOR) applications.[1–4] They act as rheology modifiers to alter the viscosity of the continuous phase, improve the mobility ratio and sweep efficiency, and increase recovery and oil production rates. The polymer system must withstand the serve conditions in the oil reservoir. In addition, the polymer is supposed to provide complete solubility, exhibit high viscosity at low solution concentration, low interfacial tension with regard to the oil phase, and good mobility control.[5] The polymer also should be inexpensive.

Correspondence to: B. Nyström (bo.nystrom@kjemi.uio.no).

Contract grant sponsor: VISTA/Statoil; contract grant number: 6338.

Polymer systems of various natures are suggested for polymer flooding, such as polyacrylamides,[1,3] xanthanes,[6,7] as well as more complex polymers, mixtures of polymers,[2,6] and polymer–surfactant mixtures.[4,8] Despite these promising polymer systems for EOR, there is still along way to go to find an optimal system for the high salinities and temperatures in the reservoirs off-shore Norway, especially because these polymers, in addition to being able to show good stability at these harsh conditions, also need to be classified as environmentally friendly. A problem with most of polymers in this category is that they exhibit severe degradation over time under these conditions, and this leads to a strong reduction of the viscosity enhancement.

To overcome the weakness of solutions of conventional polymers, preparation of chemically cross-linked nanoparticles has recently attracted interest.[9–11] The idea is that particles of various sizes should enter the pores in the oil reservoir and thereby improve the displacement of the oil. Water flooding is one of the most successful and extensively used secondary recovery methods. In this process, water is injected under pressure into the reservoir via injection wells and drives the oil through the rock

into nearby producing wells. In this case, it can be important to enhance reservoir control, that is, to mobilize oil that may be present in less permeable areas. To accomplish this, cross-linked particles that can act as blocking agents can be injected, and as a result obstruction occurs in the high permeability channels, leading to a situation where the lower permeability paths appear more favorable to a subsequent flood.

Even when chemical cross-linking of polymers takes place in very dilute solutions, there are two possible types of cross-linking processes,[12–16] that is, inter- and intrapolymer cross-linking. The former involves a cross-linked polymer via the coupling of two or more polymer chains, and this allows for the formation of interchain complexes, whereas the latter does not alter the molecular weight of the cross-linked polymer but affects quantities related to the polymer chain dimension, because the cross-linking occurs within the same polymer chain. In this case, the size of the individual polymer coil is expected to shrink. Both cross-linking mechanisms are expected to yield particles, but the particle size and size distribution of the particles will be different. In a recent study[15] on the chemical cross-linking of hydroxyethylcellulose (HEC) in dilute aqueous solutions with divinyl sulfone (DVS) as the cross-linker agent at basic conditions (pH $\approx$ 12), it was shown that interchain cross-linking is the predominant mechanism at quiescent conditions. Dynamic light scattering (DLS) experiments revealed a rapid growth of the clusters in the course of time, and no sign of compression of the molecules could be observed. However, when a dilute reaction mixture was subjected to a shear flow, intrapolymer cross-linking with contraction of the coils was observed, and at moderate shear rates interpolymer cross-linking and the formation of aggregates followed at longer times during the cross-linking process. The growth of the multichain aggregates is reduced with increasing shear rates, and at very high shear rates no interchain cross-linking was detected.

In the present work, alkali aqueous mixtures of 0.1 wt % HEC with DVS are exposed to different shear stresses during the cross-linking reaction by introducing a mechanical stirrer into the reaction mixture and applying different rotational speeds. The contraction and growth of clusters in the reaction mixture under the influence of different shear flows are characterized with the aid of turbidimetry, DLS, and rheo-small-angle light scattering (rheo-SALS) at various stages in the course of the cross-linking process by quenching the mixture to a lower pH value (pH $\approx$ 2) by adding a few drops of concentrated HCl. In this way, the reaction is terminated immediately. In the experimental series, small amounts of the reaction mixture were continuously taken out and rapidly quenched, and measurements were carried out on samples taken out at different times during the cross-linker reaction.

In this work, we demonstrate that cross-linked particles of various sizes can be prepared by conducting chemical cross-linking of a dilute polymer solution at various stirring speeds. The results show that the size of the cross-linked particles can be tuned by quenching the reaction mixtures at different times and applying various stirring speeds during the cross-linking process. The stability of these species at diverse cross-linker times and stirring speeds is also investigated. These findings can be utilized in the preparation of cross-linked particles of desired sizes.

EXPERIMENTAL

Materials and solution preparation

In this work, we used a hydroxyethylcellulose (HEC) sample with the trade name Natrosol 250 GR (lot. no. A-0382) that was provided by Hercules, Aqualon Division (Wilmington, DE). The degree of substitution of hydroxyethyl groups per repeating anhydroglucose unit of the polymer is 2.5 (given by the manufacturer). The weight-average molecular weight (M_w = 400,000) and the overlap concentration (c^* = 0.25 wt %) of this HEC sample in aqueous solution have both been reported previously.[15] To remove salt and other low-molecular-weight impurities, dilute HEC solutions were dialyzed against Millipore water for 7 days and recovered by freeze drying. Regenerated cellulose with a molecular weight cutoff of $\approx$ 8,000 (Spectrum Medical Industries, Rancho Dominguez, CA) was employed as dialyzing membrane. The cross-linking agent DVS was purchased from Merck (Darmstadt, Germany) and used without further purification. Millipore water was utilized for the preparation of all solutions.

All solutions were prepared by weighing the components and Millipore water was always used. After freeze-drying, HEC was redissolved in 0.05*M* NaOH (pH $\approx$ 12; alkaline conditions are necessary for the cross-linker reaction to proceed) solution with a fixed polymer concentration of 0.1 wt % (this concentration is far below the overlap concentration), and the solution was homogenized by stirring at room temperature for 1 day. All experiments were carried out at 25°C or room temperature.

Asymmetric flow field-flow fractionation

The asymmetric flow field-flow fractionation (AFFFF) experiments were carried out on an AF2000 FOCUS system (Postnova Analytics, Landsberg, Germany) equipped with an RI-detector (PN3140,

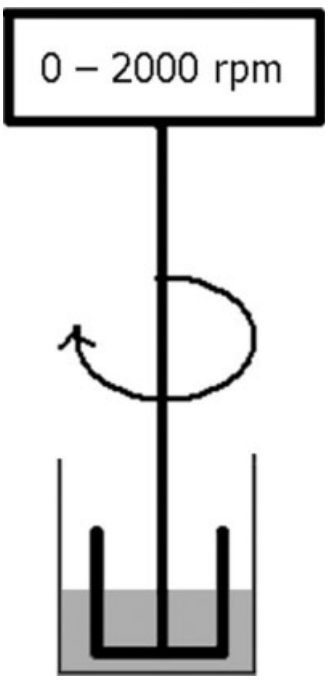

Figure 1 Sketch of the geometry of the mechanical stirrer.

Postnova) and a small-angle (seven detectors in the range 35°–145°) light scattering detector (PN3070, $\lambda = 635$ nm, Postnova). Measurements were performed on HEC samples (0.1 wt % samples, quenched from the reaction mixtures at various stages in the course of the cross-linking process) by using a 250-μm spacer, a regenerated cellulose membrane with a molecular weight cutoff of 10,000 (Z-MEM-AQU-427N, Postnova), and an injection volume of 20 μL. The measurements were conducted utilizing a constant detector flow rate of 0.2–0.8 mL/min and a slot-pump flow rate of 0.8–0.2 mL/min (the sum of the slot-pump flow rate and the detector flow rate was always 1.0 mL/min). The focusing time was 15 min at a cross-flow of 2 mL/min. Thereafter, the cross-flow was reduced linearly to 0.3 mL/min during a 3-min period. The cross-flow was then reduced exponentially (exponent of 0.3) to zero during a period of time of 7 min. Processing of the measured data was accomplished by the Postnova software (AF2000 Control, version 1.1.0.11). Information about the molecular weight of the samples at different stages was obtained using this software with a Zimm fit.

Rheological experiments

To apply various shear forces on the reaction mixtures, a mechanical stirrer device of the type IKA EUROSTAR power control-visc was purchased from IKA®-Werke Gmbh & Co. KG, Germany. A principal sketch of the experimental set-up with the mechanical stirrer is displayed in Figure 1. The beaker was filled with 100 mL 0.1 wt % HEC aqueous alkaline solution and the sample was exposed to a preset rotational speed in the range 0–400 rpm, and 15 μL/g of DVS was added to the solution to start the cross-linker reaction. For the sample with 0 rpm, a fast homogenization of the solution was performed (5 min at 50 rpm) before the stirrer was turned off. The cross-linker reaction in solutions of the polymer occurs between the cross-linker molecules and hydroxyl groups on the polymer chains.

At different times during the reaction at a prescribed rotational speed, 4 mL was withdrawn from the reaction mixture with a pipette, and this test sample was quenched rapidly by adding a few drops of concentrated HCl to the sample to lower the pH to acid conditions (pH $\approx$ 2) and thereby the cross-linker reaction was terminated. The same procedure to prepare the test solutions was repeated at all stirring speeds to ensure good reproducibility of the measurements.

Turbidimetry

Transmittances of quenched 0.1 wt % alkali solutions of HEC, exposed to different stirring speeds, at various stages during the cross-linker reaction were measured with the aid of a temperature-controlled Helios Gamma (Thermo Spectronic, Cambridge, UK) spectrophotometer at a wavelength of 500 nm. The apparatus is equipped with a temperature unit (Peltier plate) that gives a good temperature control over an extended time. The turbidities τ of the solutions were determined from the relation: $\tau = (-1/L)\ln(I_t/I_0)$, where L is the light path length in the cell (1 cm), I_t is the transmitted light intensity, and I_0 is the incident light intensity. The cloud point (CP) of a sample was determined as the temperature at which the first deviation from the baseline occurred.

Dynamic light scattering

The DLS experiments were conducted by means of an ALV/CGS-8F multi-detector compact goniometer system, with 8 off fiber-optical detection units, from ALV-GmbH, Langen, Germany. The beam from a Uniphase cylindrical 22 mW He-Ne-laser, operating at a wavelength of 632.8 nm with vertically polarized light, was focused on the sample cell (10-mm NMR tubes) through a temperature-controlled cylindrical quartz container (with 2 plane-parallel windows), vat (the temperature constancy being controlled to within ±0.01°C with a heating/cooling circulator), which is filled with a refractive index matching liquid (*cis*-decalin). The polymer solutions were filtered through 5-μm filter (Millipore) directly into precleaned NMR tubes.

In the DLS measurements, the intensity correlation function was measured at eight scattering angles simultaneously in the range 22°–141° with 4 ALV5000/E multiple-τ digital correlators. In the dilute concentration regime probed in this study, the scattered field obeys Gaussian statistics and the measured correlation function $g^2(q,t)$, where $q = (4\pi n/\lambda)\sin(\theta/2)$, with λ, θ, and n being the wavelength of the incident light in a vacuum, the scattering angle, and the refractive index of the medium, respectively, can be related to the theoretically amenable first-order electric field correlation function $g^1(q,t)$ by the Siegert relationship[17] $g^2(q,t) = 1 + B\,|\,g^1(q,t)\,|^2$, where B is usually treated as an empirical factor.

The correlation functions can be described by the sum of a single exponential and a stretched exponential[15]

$$g^1(t) = A_f \exp\left(-t/\tau_f\right) + A_s \exp\left\lfloor -(t/\tau_{se})^{\beta}\right\rfloor, \quad (1)$$

with $A_f + A_s = 1$. The parameters A_f and A_s are the amplitudes for the fast and the slow relaxation times, respectively. The variables τ_f and τ_{se} are the relaxation times characterizing the fast and the slow relaxation processes, respectively. This type of bimodal relaxation process has been reported[15,18,19] from DLS studies on aggregating polymer systems of various natures. In the analysis of the correlation functions by means of eq. (1), a nonlinear fitting algorithm was employed to obtain best-fit values of the parameters A_f, τ_f, τ_{se}, and β appearing on the right-hand side of eq. (1).

The fast mode is diffusive (q^2-dependent) for all the samples, and it yields the mutual diffusion coefficient $D(\tau_f^{-1} = Dq^2)$ of molecularly dispersed species and small aggregates. The slow mode [the second term on the right-hand side of eq. (1)] characterizes the dynamics of large aggregates and this mode is also always found to be diffusive.

The parameter τ_{se} in eq. (1) is some effective relaxation time, and β ($0 < \beta \leq 1$) is a measure of the width of the distribution of relaxation times. The mean relaxation time for the slow mode is given by

$$\tau_s = \frac{\tau_{se}}{\beta}\Gamma\left(\frac{1}{\beta}\right), \quad (2)$$

where Γ is the gamma function. The values of β are in the interval $0.6 < \beta < 0.95$ in this study. The general trend is that the value of β becomes larger at a later stage of the cross-linking process. This indicates a narrower size distribution of species at a later stage of the cross-linking process.

Since both the relaxation modes are found to be diffusive, this enables us to calculate the apparent hydrodynamic radii ($R_{h,f}$, and $R_{h,s}$) from the fast and slow relaxation times, respectively, via the Stokes-Einstein relationship $D = k_BT/6\pi\eta R_h$, where k_B is the Boltzmann constant, T is the absolute temperature, η is the solvent viscosity, and D is the diffusion coefficient of the species in the solution.

Rheo-small-angle light scattering measurements

Combined rheological and small angle light scattering (rheo-SALS) experiments during shear flow were performed simultaneously using the Paar-Physica MCR 300 rheometer, equipped with a specially designed parallel plate-plate configuration (the diameter of the plate is 43 mm) in glass.[20] The instrumentation for the rheo-SALS experiments was purchased from Physica-Anton Paar (Graz, Austria). In all measurements, a 10-mW diode laser operating at a wavelength of 658 nm was used as the light source; a polarizer was placed in front of the laser and an analyzer below the sample, making both polarized (polarizer and analyzer parallel) and depolarized (polarizer and analyzer perpendicular) experiments possible. All experiments in this study were conducted using polarized light scattering. Utilizing a prism, the laser beam was deflected and passed through the sample placed between the transparent parallel plates. The distance between the plates was small (0.5 mm), so that the effect of multiple scattering was less pronounced when the sample became turbid at long cross-linker times. The light propagated along the velocity gradient direction, thus probing the structure in the plane of flow and vorticity. The forward scattered light at small angles was collected on a flat translucent screen below the sample (distance between sample and screen was 12.3 cm).

The 2D scattering patterns formed on the screen were captured using a CCD camera (driver LuCam V. 3.8), whose plane is parallel to that of the screen. A Lumenera (VGA) CCD camera (Lumenera Corporation, Ottawa, Canada) with a Pentax lens was utilized, and the scattered images were stored on a computer using the StreamPix (NorPix, Montreal, Quebec, Canada) application software (version 3.18.5), which enables a real-time digitalization of the images. The images were acquired via the CCD camera with an exposure time of 200 ms. Subsequently, the pictures were analyzed using the SALS-software program (version 1.1) developed by the Laboratory of Applied Rheology and Polymer Processing, Department of Chemical Engineering, Katholieke Universiteit Leuven, Leuven, Belgium. The scattering functions were recorded continuously during the run. The approximate accessible scattering wave vector (q) range is between $q = 4 \times 10^{-4}$ nm^{-1} and $q = 2 \times 10^{-3}$ nm^{-1}.

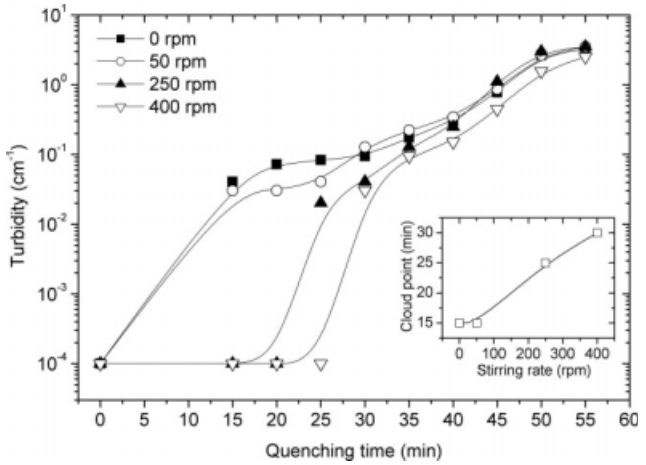

Figure 2 Turbidity at different stages during the cross-linking of 0.1 wt % solutions of HEC in the presence of 15 μL/g DVS at the stirring speeds indicated. The inset plot shows the values of the cloud point determined from the incipient rise of the turbidity curve.

RESULTS AND DISCUSSION

Turbidity

In the course of the cross-linker process, the growth of large interpolymer aggregates increases the turbidity of the solution. In this way, the turbidity can be used as an indicator of the level of interchain cross-linking. Figure 2 shows that in the course of the cross-linker reaction of a 0.1 wt % HEC solutions in the presence of 15 μL/g of the cross-linker DVS, the samples become turbid. The results indicate that the formation of large aggregates is postponed to later times when the sample is exposed to higher stirring speed during the cross-linker reaction. The inset demonstrates that the cloud point time increases as the shear flow increases. This finding suggests that interchain association is delayed because shear forces make it more difficult for the chains to form interpolymer contacts. However, when most of the intramolecular cross-linking sites have been consumed, the frequent collision of the molecules leads to the formation of large aggregates. Actually, at long reaction times, the impact of rotational speed on the turbidity is modest.

Dynamic light scattering and AFFFF

Normalized correlation function data at a scattering angle of 124° for aqueous 0.1 wt % HEC solutions at various stages in the course of the cross-linker reaction performed at two different stirring speeds, together with one solution without DVS (0 min), are depicted in the form of semilogarithmic plots in Figure 3. The general behavior is that the relaxation function is shifted toward longer times as the cross-linking process proceeds, and this trend is less pronounced with increasing stirring speed. The slower decay of the correlation function at long times reflects the growth of large clusters.

In connection with EOR applications, it is important that the particles are stable over an extended temperature domain. By plotting the correlation function data against the quantity tT/η_0 (where T is the absolute temperature and η_0 is the solvent viscosity), trivial changes of the solvent viscosity with the temperature have been taken into account. Since the correlation data at all temperatures virtually condense onto each other, the effect of temperature on the diffusion behavior of the particles can be neglected [see Fig. 3(c)].

To scrutinize the goodness of the fitting procedure and to endorse the functional form of the fitting algorithm [eq. (1)] that was employed to portray the correlation functions, residual plots from the fittings

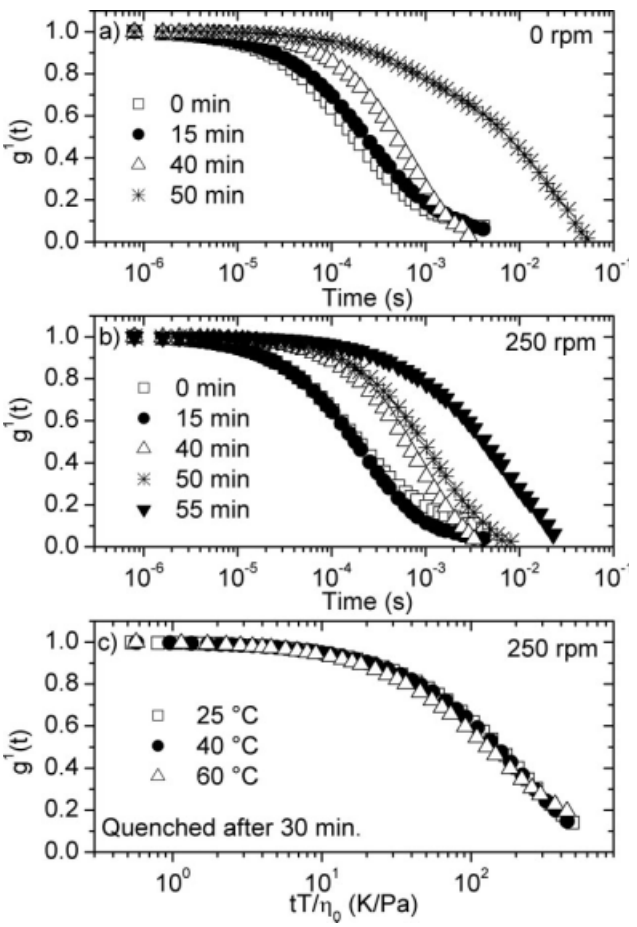

Figure 3 (a, b) Plot of the first-order electric field correlation function versus time (every second data point is shown) at a scattering angle of 124° for 0.1 wt % HEC solutions without and with cross-linker at various stages during the cross-linking reaction and for samples at two different rotational speeds (0 and 250 rpm). (c) Plot of $g^{(1)}(t)$ versus the quantity tT/η_0 for cross-linked particles in 0.1 wt % HEC at the temperatures indicated.

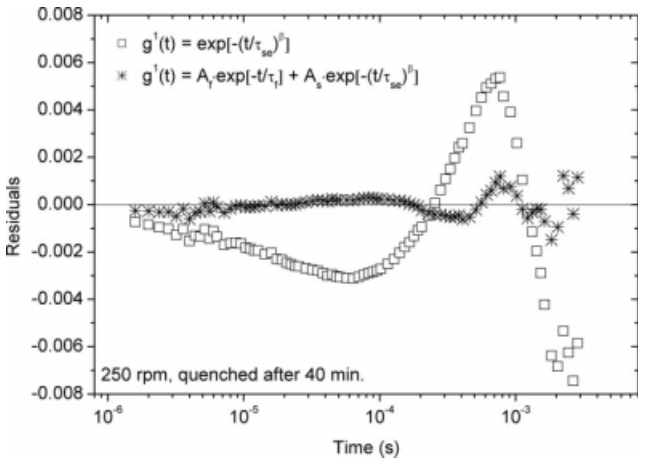

Figure 4 Plot of the residuals by fitting a typical correlation function with the aid of one stretched exponential or eq. (1). See text for details.

of a typical correlation function by using a single stretched exponential or eq. (1) are displayed in Figure 4. By fitting the correlation function by means of a single stretched exponential [the last term of eq. (1)], it is evident that the corresponding values of the residuals are large and the residual curve exhibits a systematic trend. This is a signature of that this is a poor fit of the data. The random distribution and small values of the residuals by fitting the correlation function data with the aid of eq. (1) indicate good agreement between the fitting expression and the data. This suggests a bimodal form of the correlation function as specified by eq. (1), where the fast mode portrays the diffusion behavior of the molecularly dispersed entities or small clusters, whereas the slow mode depicts motions of the large aggregates. Although the population of the huge complexes dominates at the later stage of the cross-linker reaction, we were able in all instances to separate the contribution from the smaller species.

The analysis of the correlation functions unveil that both relaxation modes are diffusive, and by using the Stokes-Einstein relationship, the apparent hydrodynamic radii of the fast ($R_{h,f}$) and the slow ($R_{h,s}$) modes can be calculated. The results are depicted in Figure 5. It is obvious that at early times during the cross-linking process, the fast mode yields low values of $R_{h,f}$ but at later stages of the cross-linker reaction, higher values of $R_{h,f}$ are observed. At later times in the course of the cross-linker reaction, the number of molecularly dispersed units gradually become smaller and the population of minute clusters affect the fast relaxation time. The growth of these clusters is delayed to longer reaction times when the quenched solutions are exposed to increasing stirring speeds.

The apparent hydrodynamic radius $R_{h,s}$, calculated from the slow relaxation time, represents the population of larger aggregates in the solution [Fig. 5(b)]. It is interesting to note that at early times in the course of the cross-linking process, the clusters contract, and this phenomenon becomes significantly stronger for the sample that has been subjected to the highest stirring speed. This clearly shows that initially the larger complexes depicted by the slow relaxation mode are exposed to intrapolymer cross-linking, and this feature is strengthened under the influence of shear forces because this perturbation reduces the tendency to form interchain aggregates. This behavior is consistent with the shear viscosity results reported[15] for this system previously. At later times in the course of the cross-linker reaction, larger aggregates are formed, probably because most of the sites for intramolecular cross-linking have been consumed and the repeated collisions between the species have provoked interchain cross-linking. However, high shear stresses repress the tendency of forming massive aggregates even at long reaction times. These findings plainly reveal that a dilute polymer solution with a cross-linker agent is less disposed to build up interpolymer cross-links under the influence of vigorous stirring.

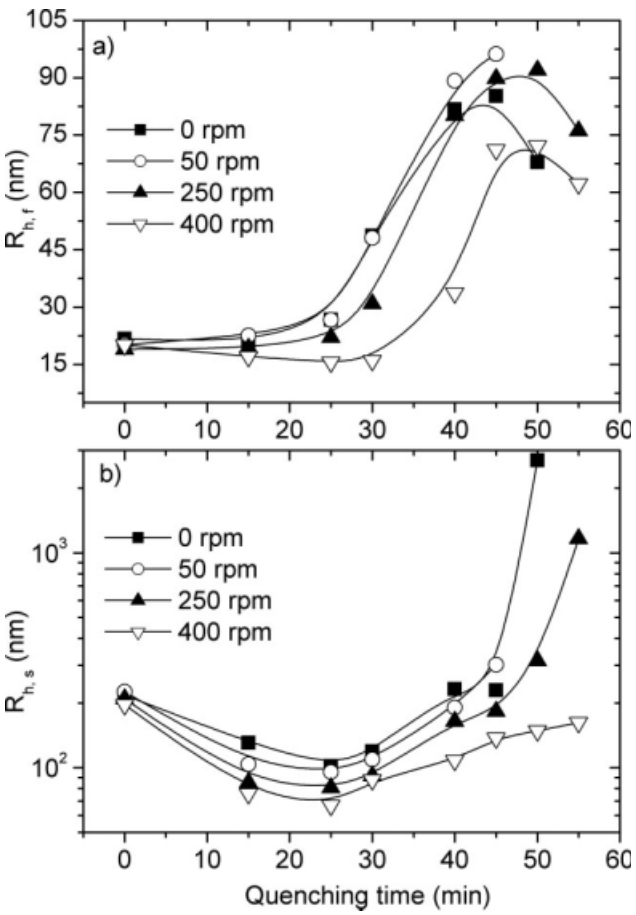

Figure 5 Effects of stirring speed on the apparent hydrodynamic radii, determined from the fast mode ($R_{h,f}$) and the slow mode ($R_{h,s}$), for 0.1 wt % solutions of HEC at various stages during the cross-linking process.

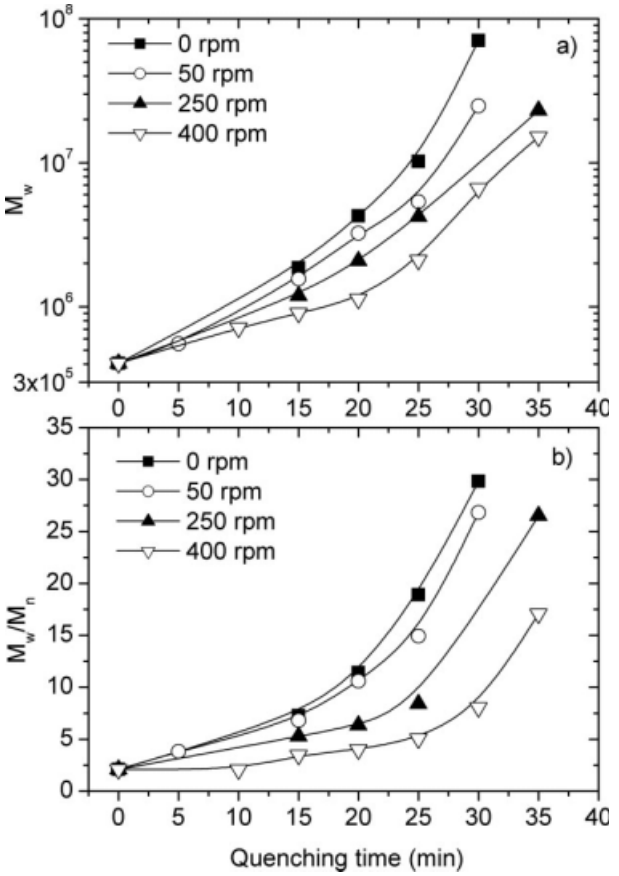

Figure 6 Time evolution of the molecular weight and the polydispersity index determined from AFFFF for 0.1 wt % HEC solutions at various stages during the cross-linker reaction and under the influence of different stirring rates.

Figure 6 shows the effects of reaction time and stirring rate on the weight-average molecular weight and the polydispersity index (M_w/M_n) for 0.1 wt % HEC solutions. This information is usually difficult to obtain, but with the aid of AFFFF it is possible to gain insight into these features. It is evident from Figure 6(a) that the molecular weight increases in the course of the cross-linker reaction. This feature suggests that giant interpolymer complexes are formed as the reaction proceeds, but as discussed above, the growth of these clusters is repressed under the influence of a high stirring speed. This finding is compatible with the results from DLS. The coexistence between the formation of intrachain and interchain cross-links during the cross-linker reaction is expected to yield species of various sizes. This is supported by the results in Figure 6(b), but higher stirring speeds seem to produce species with much less polydispersity. This can probably be ascribed to disintegration of very large aggregates at high shear flows, and this yields a more narrow distribution of sizes. These results indicate that a high stirring speed yields both smaller aggregates and less polydispersity.

Rheo-SALS

This type of technique can provide us with information about structural changes of cross-linked complexes on a global dimensional scale under the influence of shear flow. By this experimental method, it is possible to monitor shear-induced aggregation or disintegration of species in situ. Figure 7 illustrates

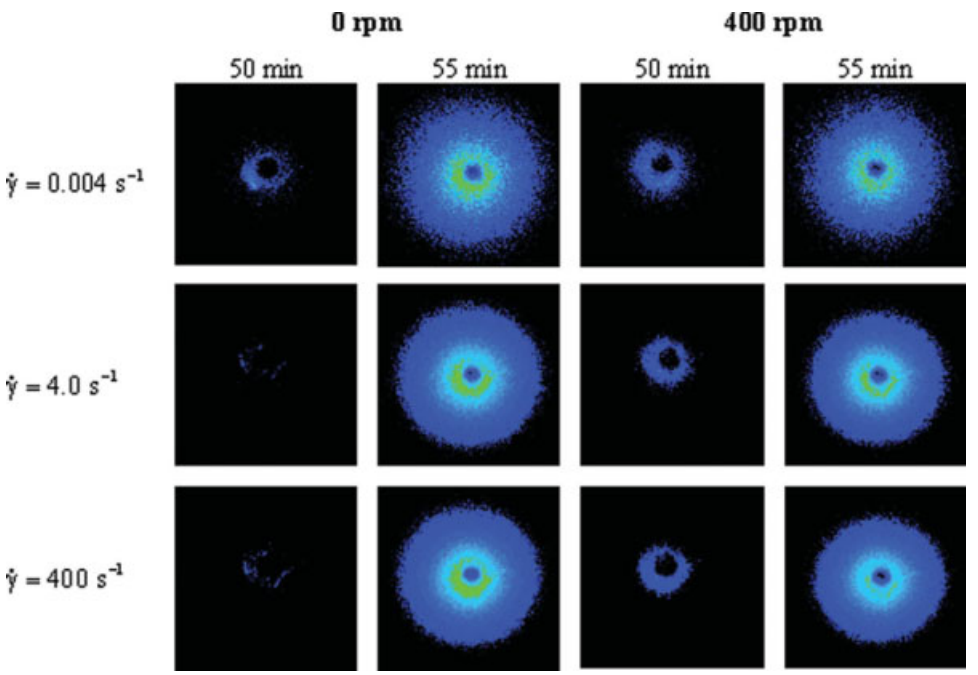

Figure 7 2D SALS patterns at various shear rates of 0.1 wt % HEC solutions at different stages during the cross-linker reaction of mixtures exposed to two different stirring speeds. [Color figure can be viewed in the online issue, which is available at www.interscience.wiley.com.]

the 2D patterns of the scattered intensity at different shear rates and cross-linking stages for 0.1 wt % HEC solutions that have been exposed to various stirring speeds during the cross-linking process. For the solution in the quiescent state that has been quenched after 50 min, the species are broken up under the influence of shear rate, whereas more shear-rate-stable clusters are evolved after 50 min when the reaction mixture was subjected to a high stirring speed. At this stage of the cross-linker reaction, the high collision frequency of the polymer entities seems to build up multichain aggregates that are more stable against mechanical stresses. After a sufficiently long cross-linker reaction period, the scattered intensity is strong and huge aggregates are formed, both for the solution in the quiescent state and for the solution exposed to a high stirring rate. These association complexes are practically not affected by either shear stresses or stirring speeds. In the considered wave vector range, most of the SALS patterns are virtually isotropic, which suggests that on this dimensional scale, no major structural alterations occur.

To elucidate the impact of shear flow on the formation of structures at various stages in the course of the cross-linking process, shear rate dependences of the scattered intensity (at a fixed q value of 0.27 μm^{-1}) for 0.1 wt % solutions of HEC in the presence 15 μL/g DVS that have been exposed to a constant stirring speed of 250 rpm are depicted in Figure 8(a). For the HEC solution (0.05*M* NaOH) without DVS, the scattered intensity is practically unaffected by the shear flow, which indicates that no significant structural changes of the molecules occur. The moderate upturn of the scattered intensity at high shear rate is ascribed to incipient turbulence. For solutions at early states of the cross-linker reaction, the scattered intensity drops at higher shear rates. As the cross-linking process advances, the intensity at low shear rates increases and the intensity falls off at higher shear rates. This scenario suggests that aggregates are broken up at higher shear stresses, whereas stronger association complexes are formed as the cross-linker reaction proceeds. Actually, when massive aggregates have been formed, the intensity is virtually unaltered, with increasing shear flow over the considered shear rate interval. This finding supports the conjecture that more sturdy complexes are formed at a later state during the cross-linking process.

A comparison of the effect of stirring speed on the scattered intensity during the cross-linker reaction for 0.1 wt % HEC solutions at two different times of quenching is depicted in Figure 8(b,c). At the earlier state of quenching, the species from the reaction mixture that has been subjected to a lower stirring speed are disintegrated at a high shear rate, whereas virtually no alteration of the scattered intensity with

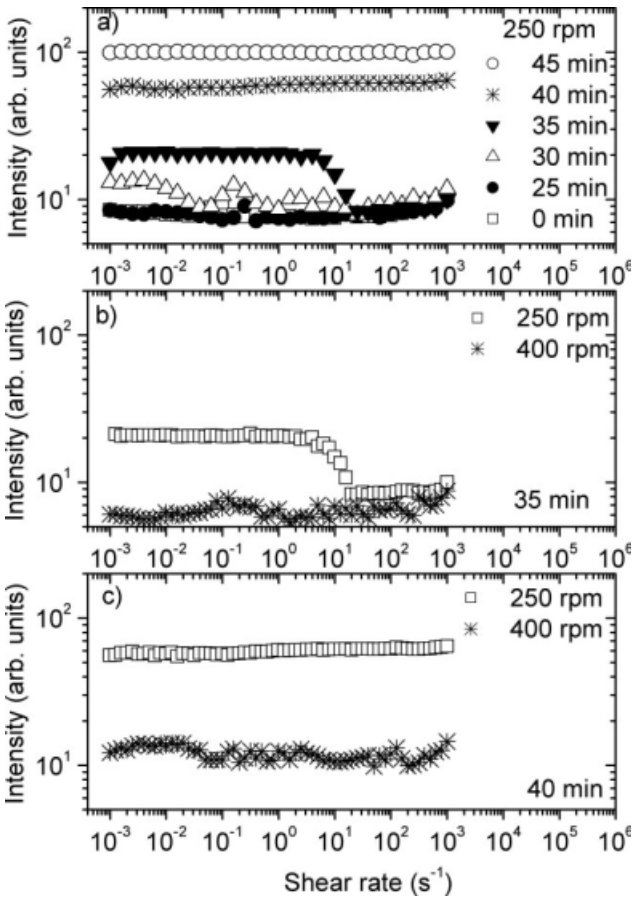

Figure 8 (a) Shear rate dependences of the scattered intensity (at a fixed *q* value of 0.27 μm^{-1}) at different stages during the cross-linker reaction (15 μL/g DVS) for 0.1 wt % solutions of HEC that have been subjected to a stirring speed of 250 rpm in the course of the cross-linking process. (b,c) Effects of shear rate and stirring speed on the scattered intensity at two different stages in the course of the cross-linking process.

increasing shear rate occurs for the sample exposed to a higher stirring speed. This finding supports the idea that the more intense collision of species at a higher stirring speed leads to compacter objects that are less disposed to breakup under the influence of shear stresses. At a later state of the cross-linking process [Fig. 8(c)], the scattered intensity is independent of shear rate at both stirring speeds. This observation indicates that as the cross-linker reaction proceeds, more stable aggregates are formed that can withstand the applied shear forces.

CONCLUSIONS

In the present work, dilute HEC solutions have been chemically cross-linked at alkaline conditions under the influence of different stirring speeds; at various stages during the cross-linking process, the reaction was terminated by quenching the mixture to an acid pH. The results demonstrate that cross-linked

particles are produced with a broad size distribution. In the course of cross-linking of polymer chains in the dilute concentration regime, competition between intrachain and interchain cross-linking is an omnipresent phenomenon. It has been shown that when dilute HEC solutions are exposed to high stirring speeds during the cross-linking process, the growth of large aggregates is suppressed. The results from AFFFF sustain this finding, and it is also found that the molecular weight polydispersity of the species is less at high stirring speeds.

It is observed from the DLS measurements that high stirring speeds at early states of the cross-linker reaction promote intrapolymer cross-linking, with contraction of polymer species, and reduction of the growth of aggregates at long reaction times. The sizes of the particles are virtually not affected by temperature in the interval 25–60°C.

The results from the rheo-SALS experiments disclosed that at early times during the cross-linker reaction, the complexes are fragile against shear forces if the reaction mixture had been subjected to low stirring speeds. However, high stirring speed of the reaction mixture in the course of the cross-linking process generates stronger aggregates because of a more efficient packing of the chains in the complexes. At a later state of cross-linking, more cross-links lead to better stability of the species even for solutions that have been exposed to low stirring speeds during the cross-linking process. This work has demonstrated that particles of various sizes can be prepared by exposing the solutions to different stirring speeds during the cross-linker reaction and to terminate the reaction at desired reaction times. This opens the possibility for preparation of particles that can be used for enhanced oil recovery applications.

References

1. Hou, J.; Liu, Z.; Zhang, S.; Yue, X.; Yang, J. J Petrol Sci Eng 2005, 47, 219.
2. Sabhapondit, A.; Borthakur, A.; Haque, I. Energ Fuel 2003, 17, 683.
3. Ghannam, M.; Esmail, N. J Appl Polym Sci 2002, 85, 2896.
4. Kjøniksen, A.-L.; Beheshti, N.; Kotlar, H. K.; Zhu, K.; Nyström, B. Eur Polym J 2008, 44, 959.
5. Chelaru, C.; Diaconu, I.; Simionescu, I. Polym Bull 1998, 40, 757.
6. Mothe, C. G.; Correia, D. Z.; de Franca, F. P.; Riga, A. T. J Therm Anal Calorim 2006, 85, 31.
7. Audibert, A.; Noik, C.; Lecourtier, L. J Can Pet Technol 1993, 32, 53.
8. Babadagli, T. Colloids Surf A 2003, 223, 157.
9. Snowden, M. J.; Vincent, B.; Morgan, J. C. U.K. Pat. GB 226 2117A (1993).
10. Ju, B.; Fan, T.; Ma, M. China Particuol 2006, 4, 41.
11. Aalaie, J.; Rahmatpour, A. J Macromol Sci Phys 2008, 47, 98.
12. Ulanski, P.; Bothe, E.; Rosiak, J. M.; Sonntag, C. Macromol Chem Phys 1994, 195, 1443.
13. Wang, B.; Mukataka, S.; Kodama, M.; Kokufuta, E. Langmuir 1997, 13, 6108.
14. Schmitz, K. S.; Wang, B.; Kokufuta, E. Macromolecules 2001, 34, 8370.
15. Maleki, A.; Kjøniksen, A.-L.; Nyström, B. J Phys Chem B 2005, 109, 12329.
16. Liu, Z.; Maleki, A.; Zhu, K.; Kjøniksen, A.-L.; Nyström, B. J Phys Chem B 2008, 112, 1082.
17. Siegert, A. J. F. Radiation Laboratory Report Number 465; Massachusetts Institute of Technology, Cambridge, MA, 1943.
18. Kjøniksen, A.-L.; Nyström, B.; Lindman, B. Langmuir 1998, 14, 5039.
19. Lauten, R. A.; Nyström, B. Colloids Surf A 2003, 219, 45.
20. Zhu, K.; Jin, H.; Kjøniksen, A.-L.; Nyström, B. J Phys Chem B 2007, 111, 10862.